JACS
JOURNAL OF THE AMERICAN CHEMICAL SOCIETY
Article
pubs.acs.org/JACS

# Synthesis of Ladder-Type Thienoacenes and Their Electronic and Optical Properties

Tianyue Zheng,[†] Zhengxu Cai,[†] Rosina Ho-Wu,[‡] Sung Hei Yau,[‡] Valerii Shaparov,[†] Theodore Goodson, III,*[,‡] and Luping Yu*[,†]

[†]Department of Chemistry and the James Franck Institute, The University of Chicago, 929 East 57th Street, Chicago, Illinois 60637, United States

[‡]Department of Chemistry and Department of Macromolecular Science and Engineering, University of Michigan, Ann Arbor, Michigan 48109, United States

Supporting Information

**ABSTRACT:** A series of ladder-type thienoacenes based on benzo[1,2-*b*:4,5-*b*′]dithiophene (BDT) have been synthesized and characterized. They were shown to be p-type semiconductors with wide band gaps and able to support multiple stable cationic states. As the conjugation lengthens, these oligomers become more emissive, showing high quantum yields. They were shown to be good two-photon absorbers, exhibiting high two-photon absorption coefficients.

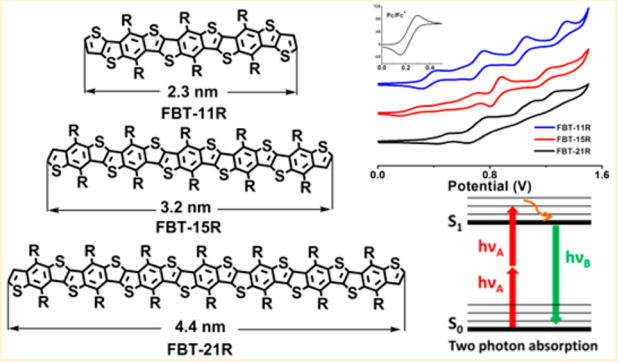


## INTRODUCTION

It is well-known that the charge transport through organic materials is strongly influenced by $\pi-\pi$-stacking interactions.[1,2] Ladder-type conjugated molecules, in which the $\pi$ systems are locked into a planar structure, thus eliminating the bond twisting in linear conjugated polymers and enhancing the $\pi-\pi$ stacking, are an effective structure to explore materials for high mobility.[3] Ladder polymers with longer conjugation and stronger $\pi-\pi$ stacking have also been continuously investigated in the past few decades with the expectation that they will exhibit interesting electro-optic properties.[3−9] Theoretical calculations on polyacenes have predicted that when the conjugation length of the polyacene is long enough, its band gap will approach zero.[10] Of course, the dilemma is that extended fused aromatic systems, which are most likely to undergo $\pi-\pi$ stacking, are insoluble in organic solvents.[11,12] A typical example is graphite, which is insoluble in any organic solvent because of $\pi-\pi$ stacking of the graphene layers. Another closely related example is that when the number of benzene rings in polyacene systems is larger than five, the materials become very difficult to dissolve in organic solvents.[13] The same problem had been a major obstacle in the development of linear conjugated polymers, which was overcome by the introduction of flexible side chains. This strategy worked in ladder polymer systems to a certain degree.[10,14,15]

Many different types of target ladder structures have been attempted, ranging from full hydrocarbon polyacenes[14,15] to systems containing heterocyclic aromatic rings.[6,16] Small molecular ladder oligomers show interesting properties. For example, single-crystal ruberene and pentacene can reach field-effect transistor (FET) mobilities as high as 40 $cm^2\ V^{-1}\ s^{-1}$, rendering them among the best p-type organic semiconductors.[17,18] Derivatives of [1]benzothieno[3,2-*b*][1]-benzothiophene (BTBT) and its further p-extended analogue dinaphtho[2,3-*b*:2′,3′-*f*]thieno[3,2-*b*]thiophene (DNTT) can also show high charge carrier mobilities.[19−21] Nitrogen-containing acenes (azaacenes) were found to be potentially useful materials for light-emitting diodes (LEDs), sensors, and FETs.[22,23] However, most ladder polymers are insoluble and do not exhibit unique physical properties compared with the small analogues.[10,24−26] The soluble versions of the ladder polymers required drastic alteration in their structures, such as the introduction of tetrahedral centers in the backbone with bulky substituents.[27] These structural modifications defeat the original purpose to utilize the strong $\pi-\pi$ interactions. Thus, the development of new soluble ladder polymers or oligomers that exhibit desired electronic and structural properties in the solid state is still a challenging task.

In this paper, we report the synthesis and characterization of a series of soluble ladder-type thienoacenes with well-defined structures based on benzo[1,2-*b*:4,5-*b*′]dithiophene (BDT). Though these oligomers are quite large and fully conjugated,

**Received:** September 28, 2015
**Published:** December 31, 2015





DOI: 10.1021/jacs.5b10175
J. Am. Chem. Soc. 2016, 138, 868−875

they have sites available for side-chain modification to tune the properties. These oligomers with well-defined lengths represent a new class of materials and enable us to correlate various physical properties with the chain length and provide an experimental basis for future theoretical investigations.

## RESULTS AND DISCUSSION

**Synthesis of Compounds.** Scheme 1 shows the synthesis of the BDT-based thienoacenes, which involves an iterative strategy that utilizes the shorter oligomers as precursors of the longer ones. A key building block is compound **1**, which was used to couple with precursors bearing triisopropylsilyl (TIPS) end-capping groups. The crucial step of the process is the formation of aromatic C−S bonds by a cyclization reaction via an intramolecular electrophilic addition of acid-activated methyl sulfoxide to adjacent thiophene units. This is a well-known reaction and has been used to construct oligomers and polymers based on fused thiophene units in high yields by the groups of Müllen and Tsuchida,[28−33] who used a strong acid, triflic acid. In this report, milder conditions using modified Eaton's reagent (TFA/$P_2O_5$) as the acidic agent were found to carry out the cyclization reaction well, followed by demethylation of sulfonium salt intermediates.[34] For example, a nine-ring distannane (compound **7**) was used as the building block for the synthesis of a compound with 21 rings, **FBT-21R** (**F**used **B**enzo**T**hiophene **21** **R**ings). The final compound exhibits a calculated molecular length of 4.4 nm, making it one of the longest soluble thienoacenes. It is clear that this synthetic approach is potentially feasible for the synthesis of longer oligomers if proper precursors are used.

The structures of the resulting compounds were investigated and confirmed by NMR spectroscopy and MALDI-TOF mass spectrometry. For example, Figure 1 shows the partial $^1$H NMR spectra of compound **4** and the cyclized product **FBT-11R**. After cyclization, the protons in the aromatic region of **4** turned into two doublet peaks in the spectrum of **FBT-11R**, which were assigned to H3 and H4. Also, the H1 protons turned into two sets of protons, H5 and H6, corresponding to the protons in $-CH_2-$ groups of the alkoxy side chains. In addition, the H2 peaks corresponding to the protons in the methylsulfinyl goups ($-S(O)CH_3$) disappeared after cyclization, indicating the removal of the methylsulfinyl groups. The molecular weight of **FBT-11R** (calcd 1394.58 g/mol) was determined by MALDI-TOF mass spectrometry (Figure S1), which exhibited the molecular ion peak of **FBT-11R** at $m/z$ 1394.86.

**Scheme 1. Synthesis of Ladder-Type Thienoacenes**[a]

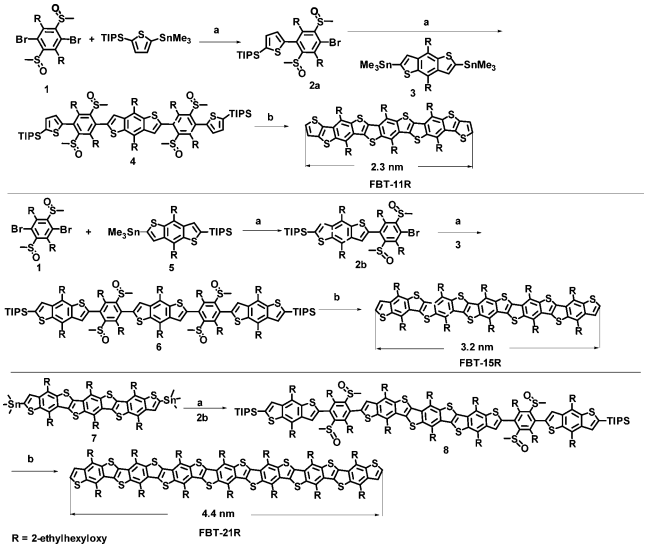


[a]Reaction conditions: (a) $Pd(PPh_3)_4$, toluene. (b) (i) $CF_3COOH/P_2O_5$; (ii) pyridine, reflux; (iii) TBAF, THF. The molecular length was calculated using DFT at the B3LYP/6-31G(d) level.

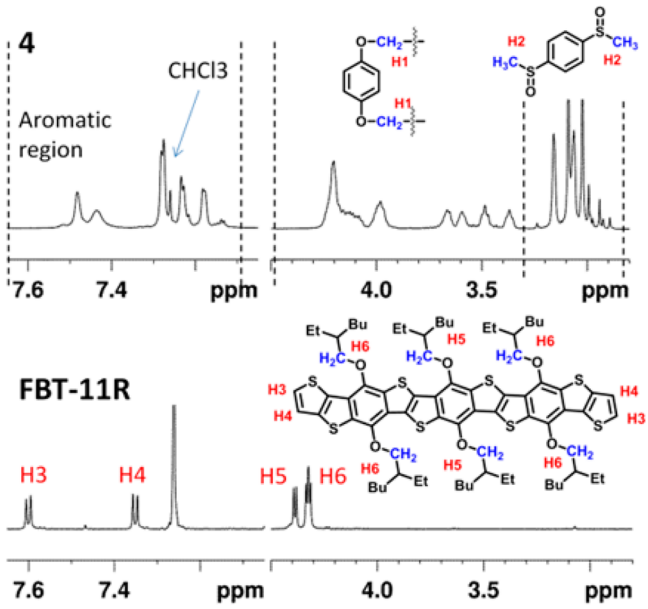


**Figure 1.** $^1$H NMR spectra of **4** and **FBT-11R**.

**Linear Optical Properties.** These thienoacene oligomers showed interesting electronic and optical properties. Their UV−vis absorption spectra showed broad absorption from 300 to 500 nm, typical acene-type absorption spectra with distinctive and narrow vibronic features (Figure 2).[35−37] A bathochromic shift in the absorption onset from 459 to 502 nm was observed as the conjugation length increased, indicating a decrease in the optical energy band gap ($E_g$) from 2.71 eV in **FBT-11R** to 2.47 eV in **FBT-21R**. The highest molar extinction coefficient ($\varepsilon$) also increased from $6.7 \times 10^4$ $M^{-1}$ $cm^{-1}$ (441 nm) for **FBT-11R** to $2.2 \times 10^5$ $M^{-1}$ $cm^{-1}$ (483 nm) for **FBT-**

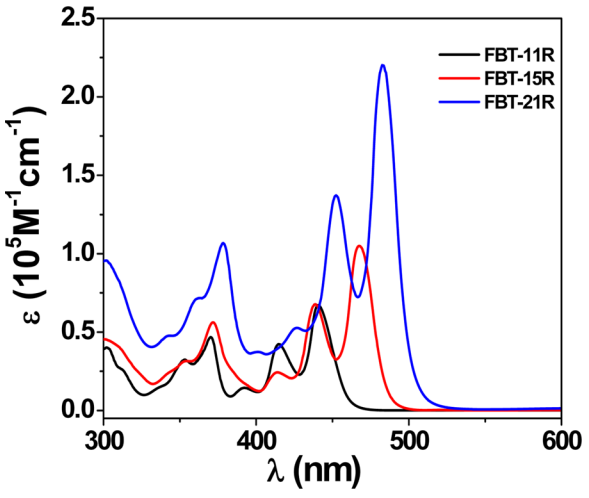


**Figure 2.** UV−vis absorption spectra of the FBT series molecules in dilute $CHCl_3$ solution.



DOI: 10.1021/jacs.5b10175
J. Am. Chem. Soc. 2016, 138, 868−875

**21R**, which was expected because of the increase in the number of aromatic units. The absorption peaks between 300 and 360 nm were similar in going from **FBT-11R** to **FBT-21R** and were independent of the conjugation length, suggesting localized excitations, possibly due to the fact that the rigid conjugation system diminished the bond rotation in the backbones of the molecules. The absorption peaks in this region can be attributed to vibronic and exciton couplings to a fundamental excitation, which progresses along the backbone of molecule. Similar vibrational progressions had been observed in rigid annulene derivatives and were assigned to a fundamental $\pi \rightarrow \pi^*$ transition and various vibronic and exciton couplings.[38]

To better understand the conformation of these molecules, geometry optimization was carried out by density functional theory (DFT) calculations. The results showed that these fully conjugated molecules adopt planar conformations (Figure S2). Therefore, C−C bond rotation was prohibited, and thus, the vibronic couplings would be mainly associated with the lengthening/shortening of the C−C bonds.

**Electrochemical Properties.** Cyclic voltammetry was also performed to measure the energy levels of these molecules. A very interesting observation was that the cyclic voltammograms (CVs) of the three ladder-type oligomers were similar, all exhibiting multiple redox peaks as shown in Figure 3.

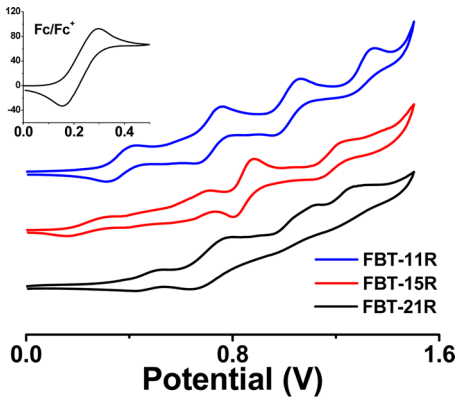


**Figure 3.** CVs of the FBT series molecules.

Compared with the CVs of nonfused conjugated molecules such as oligo(phenylene vinylene)[39−41] and oligothiophenes,[42,43] which normally show higher first oxidation potentials and fewer redox peaks, the results indicated that these compounds can be oxidized to multiple cationic states and stabilized by their large conjugation systems. For example, **FBT-11R** showed four reversible redox peaks in the region of 0−1.5 V, and the $E_{pc}/E_{pa}$ values for the four peaks were 0.43/0.31, 0.76/0.65, 1.07/0.96, and 1.35/1.27 V, respectively. However, as the molecules became larger, the redox processes became less reversible, as shown in the CVs for **FBT-15R** and **FBT-21R**, possibly because larger molecules in solution were slower when diffusing to the electrode. The results suggest that these molecules might be useful as hole-transporting materials. From the CVs, the HOMO energy levels of these oligomers were estimated to increase from −4.94 eV for **FBT-11R** to −4.82 eV for **FBT-21R**, as shown in Figure 4. The LUMO levels were deduced from the HOMO levels and the $E_g$ values obtained from UV−vis absorption onsets.

**DFT Calculations.** To further explore the effect of increasing the number of BDT units on the electron delocalization of molecules, DFT calculations were performed

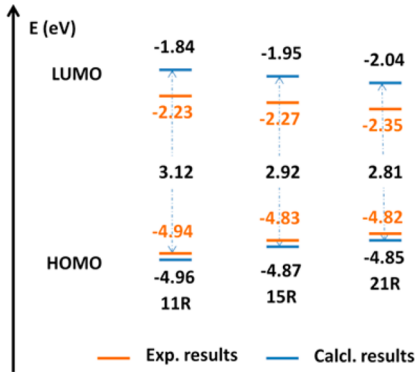


**Figure 4.** Measured energy levels of the FBT series molecules and energy levels of the FBT series molecules calculated using DFT at the B3LYP/6-31G(d) level.

on model compounds with methyl groups in place of long alkyl side chains. The calculated HOMO energy levels were consistent with the CV results. In addition, the calculation results showed that the HOMO and LUMO energy levels will eventually reach saturation as the oligomers become longer (Figure 4). This trend could also be seen in the absorption spectra, where the bathochromic shift decreased from 26 nm for going from **FBT-11R** to **FBT-15R** to 17 nm for going from **FBT-15R** to **FBT-21R**. This phenomenon was more clearly viewed by the changes in the frontier orbitals of these molecules (Figure S3). In 3- and 5-BDTs, the HOMOs/LUMOs were delocalized along the entire molecular backbones, while as the length of molecule increased, the HOMO/LUMO tended to localize in the middle of the molecule. Thus, for 13- and 15-BDTs, both the HOMO and LUMOs rarely existed on the terminal rings. Therefore, the saturation of physical properties was estimated to occur at about 15 BDT units, corresponding to 45 aromatic rings, with which an effective conjugation length (ECL) was achieved for these thienoacenes.[44] The calculation results also showed that the energy band gap of the thienoacenes could possibly be inversely proportional to their conjugation length. When the calculated $E_g$ was plotted versus the reciprocal of the conjugation length, represented by the reciprocal of the number of rings ($1/N$), a linear relationship was observed, and a saturation band gap of around 2.53 eV was therefore found (Figure S4). A similar trend has been reported for calculations on fused conjugation systems such as BTBT and DNTT derivatives and fused polythiophenes, showing that the band gap decreases as the number of fused rings increases and a linear relationship for $E_g$ versus $1/N$.[45−47] This result indicates that the corresponding polymers will be wide-band-gap semiconductors.

**Photoluminescence Properties.** Besides the absorption, the emission of the FBT oligomers was also investigated (Figure 5). A bathochromic shift of the emission maximum was observed in going from **FBT-11R** to **FBT-21R**. However, the Stokes shift showed a decreasing trend as the conjugation length increased (Table 1), suggesting that the molecules became more rigid.[48] Taking the integration of the emission signal from the spectra, the quantum yields (Q.Y., $\phi$) of these molecules were calculated to be 0.43, 0.87, and 0.87 for **FBT-11R**, **FBT-15R**, and **FBT-21R**, respectively, in chloroform (Table 1), with coumarin 307 in methanol as the reference ($\phi$ = 0.53).[49] The increase in conjugation enhanced the emission rate while the increase in the rigidity of the molecules reduced the nonradiative decay rate, and these two effects combined to


DOI: 10.1021/jacs.5b10175
J. Am. Chem. Soc. 2016, 138, 868−875

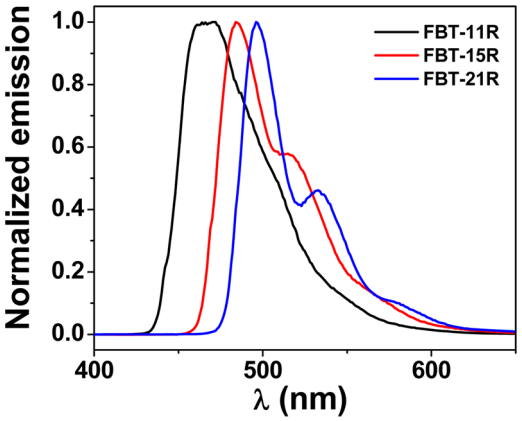


**Figure 5.** Fluorescence emission spectra of the FBT series molecules.

**Table 1. Summary of Optical Properties for the FBT Series Oligomers**

| sample | max $\varepsilon$ ($M^{-1}$ $cm^{-1}$) | $\phi$ | fluorescence lifetime (ps) | Stokes shift ($cm^{-1}$) | $\delta$ (GM) |
|---|---|---|---|---|---|
| **FBT-11R** | $6.7 \times 10^4$ | 0.43 ± 0.086 | 150 ± 10 | 1450.7 | 64 |
| **FBT-15R** | $1.0 \times 10^5$ | 0.87 ± 0.174 | 150 ± 10 | 749.0 | 72 |
| **FBT-21R** | $2.2 \times 10^5$ | 0.87 ± 0.174 | 150 ± 10 | 542.6 | 83 |

contribute to the increase in Q.Y. in going from **FBT-11R** to **FBT-21R**. Additionally, the anti geometry of the sulfur atoms in the FBT molecules prompted effective $\pi$ conjugation and contributed to the observed high Q.Y. Similar and smaller analogues of the FBT molecules based on benzothiophenes (BTs) have been previously reported.[48,50] Their emission profiles resembled those of the FBT molecules, and an increase in the Q.Y. as the conjugation became longer was also found.

Time resolved fluorescence upconversion was used to better understand the emission mechanism of the FBT molecules (Figure 6a). The emission dynamics of the FBT molecules were very similar, and the emission decays were fitted to a single-exponential function (Figure 6b). The emission lifetimes of the three molecules were found to be similar at 150 ps (Table 1), suggesting that the change in rigidity and conjugation should have little effect on the emission dynamics and that the three molecules have similar emissive states. The difference in Q.Y. is probably due to the increase in energy transferred into the emissive state as the conjugation and rigidity increase. The decrease in nonradiative states leads to a higher energy transfer efficiency and an increase in Q.Y. of these molecules.

**Two-Photon Absorption.** Further studies indicated that these molecules exhibit strong two-photon absorption, which involved the absorption of two longer-wavelength photons (800 nm) to excite the same emission state accessible by shorter-wavelength excitation (400 nm). For highly conjugated systems, it is well-known that charge delocalization and charge transfer can occur, which can be measured using two-photon techniques.[38,51−53] Compared to one-photon excitation, a red shift in the two-photon-excited emission peaks was also observed for these thienoacenes (Figure 7). The emission wavelengths of the FBT molecules are the same for one-photon and two-photon excitations. The two-photon-excited emission lacks the vibronic splitting seen in the one-photon-excited emissions because of the low spectral resolution of the two-

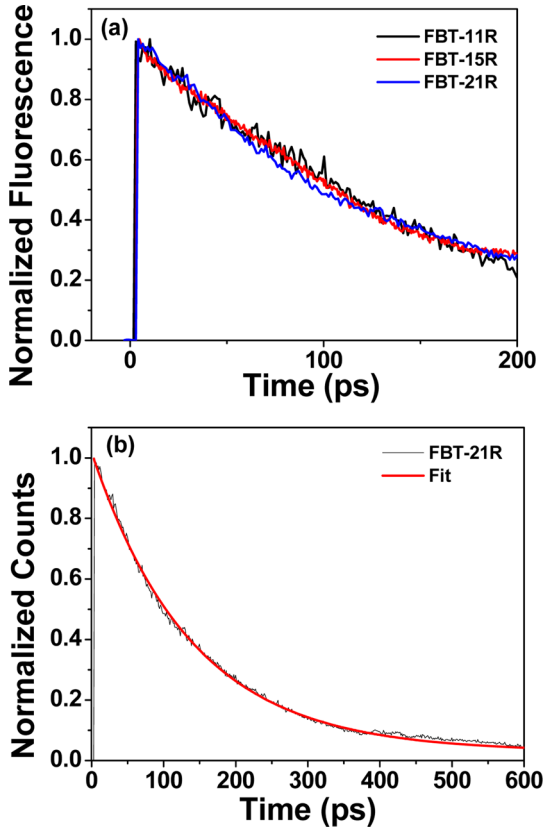


**Figure 6.** (a) Emission dynamics of the FBT series molecules. (b) Fit of the emission dynamics of **FBT-21R** to a single-exponential decay.

photon-excited fluorescence. The two-photon absorption (TPA) cross section was typically high for organic molecules,[53,54] and the cross sections of these molecules at 800 nm were calculated to be 64, 72, and 83 GM for **FBT-11R**, **FBT-15R**, and **FBT-21R**, respectively, in chloroform (Table 1), which are comparable to those of donor-$\pi$-acceptor-type compounds bearing a trivalent boron group.[55] The TPA cross section enhancement of these molecules was possibly due to the increasing conjugation and faster intramolecular charge transfer over longer molecular distance, which has been observed in branched alkene and alkyne chromophores.[51,56] However, their TPA cross sections are relatively small compared with those of other ladder-type polymers, such as poly(*p*-phenylene), which has a TPA cross section of 72 000 GM,[57] and some other linear conjugated compounds with 800 nm excitation.[58] To improve the TPA cross sections of the FBT molecules, structural modifications of both the side-chain groups and backbones may be needed to achieve more effective intramolecular charge transfer.[59,60]

## ■ CONCLUSION

A series of ladder-type thienoacenes based on BDT repeating units with extended conjugation have been synthesized by an effective acid-assisted intramolecular cyclization method. The synthetic approaches developed are versatile and enable the preparation of new thienoacene oligomers with precise structures. Optical and electrochemical characterization of these oligomers showed that they are wide-band-gap p-type semiconductors that can support multiple stable cationic states. As the conjugation increases, the band gaps of these oligomers tend to decrease and saturate. These oligomers also become


DOI: 10.1021/jacs.5b10175
J. Am. Chem. Soc. 2016, 138, 868−875

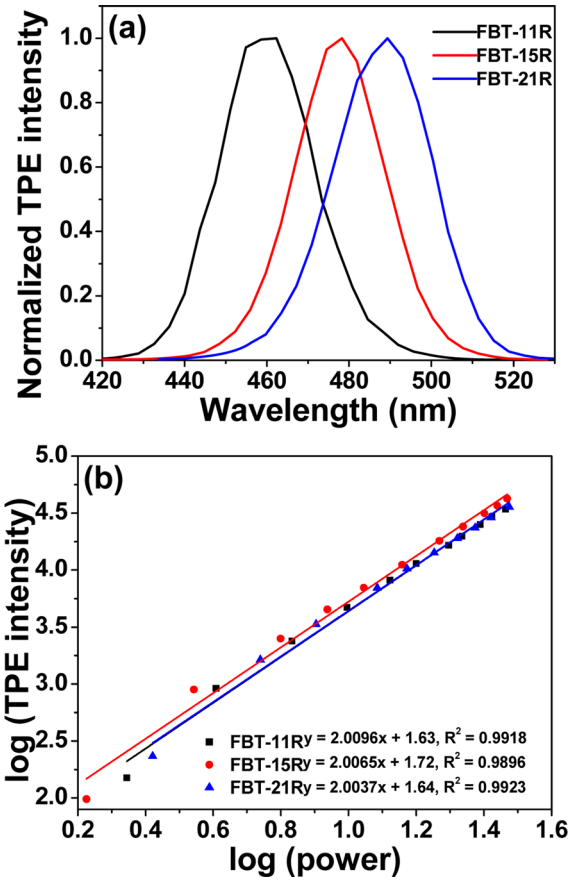


**Figure 7.** (a) Two-photon emission spectra and (b) power dependence of the two-photon-excited emission of FBT series molecules.

more emissive as the conjugation increases, showing high quantum yields and two-photon absorption coefficients.

## EXPERIMENTAL SECTION

**Materials and Instrumentation.** Unless otherwise stated, all chemicals obtained from commercial suppliers were used without further purification. All solvents were purified with a standard distillation procedure prior to use. All reactions were carried out under an argon atmosphere. NMR spectra were recorded on a 500 MHz Bruker DRX-500 spectrometer in $CDCl_3$ or $C_2D_2Cl_4$ with tetramethylsilane as an internal reference; chemical shifts ($\delta$) are reported in parts per million. Mass spectra were obtained on a Bruker Daltonics UltrafleXtreme MALDI-TOF system with a reflective positive method using dithranol as the matrix. High-resolution mass spectrometry (HRMS) was performed on an Agilent 6224 Tof-MS system. Column chromatography was carried out on silica gel (silica 60M, 400−230 mesh).

**Characterizations.** Cyclic voltammetry was used to study the electrochemical properties of these thienoacenes. They were measured as $10^{-5}$ M solutions in anhydrous $CH_2Cl_2$ containing 0.1 M $Bu_4NPF_6$ as the electrolyte with glassy carbon as the working electrode, $Ag/Ag^+$ as the reference electrode, and a Pt wire as the contrast electrode at a scan rate of 50 mV/s. For calibration, the redox potential of ferrocene/ferrocenium ($Fc/Fc^+$) was measured under the same conditions and it was located at 0.15 V vs $Ag/Ag^+$. It was assumed that the redox potential of $Fc/Fc^+$ has an absolute energy level of −4.80 eV relative to vacuum.[61] The HOMO level was then calculated according to the following equation:

$$E_{HOMO} = -(\phi_{ox} + 4.65)\ \text{eV}$$

where $\phi_{ox}$ is the onset oxidation potential vs $Ag/Ag^+$.

Geometry optimizations were carried out using the Gaussian 09 program package with the DFT method at the B3LYP/6-31G(D) level.[62]

Steady-state absorption and emission measurements were performed at room temperature with a 10 mm thick quartz sample cell. The materials were dissolved in spectroscopic grade chloroform before the experiments. Optical absorption measurements were carried out using an Agilent 8432 UV−vis absorption spectrometer. Emission spectra were measured using a Fluoromax-2 fluorimeter. The quantum yields of the molecules were measured using coumarin 307 in methanol as the standard ($\phi$ = 0.53). The reference solutions were excited at 400 nm, and the emission was measured at 495 nm. The quantum yield was calculated using data at three different concentrations. The slopes of the fluorescence intensity versus concentration plots of the standard and the sample were used to calculate the quantum yield.

The two-photon absorption cross section was calculated from the two-photon-excited emission experiment.[51,54] The TPA cross section was calculated by comparison to a known standard (coumarin 307, $\delta$ = 15 GM) over a range of powers. The samples were excited using a mode-locked laser (Kapteyn-Murnane Laboratories, pumped by a Spectra Physics Millenia), and the pulsed laser was tuned to 800 nm with a pulse width of 30 fs. The emission was collected using a Hamamatsu photomultiplier tube and a photocounting unit at the maximum emission wavelength of the sample, as selected using an Oriel Cornerstone monochromator.

The time-resolved fluorescence upconversion measurements were performed according to reported procedures.[63,64] Briefly, the samples were excited with frequency-doubled light from a mode-locked Ti:sapphire laser at 400 nm. All of the samples were held in a 1 mm thick rotating sample cuvette. Fluorescence emitted from the sample was upconverted in a nonlinear crystal of barium borate (BBO) after passing through a variable-delay line. The instrument response function (IRF) has a duration of ~200 fs for visible excitation.[64,65] The energy per excitation pulse did not exceed 600 pJ for any experiment. Standard dyes were used to calibrate the system. Lifetimes of the fluorescence decay were obtained by fitting the experimental profiles with multiexponential decay functions convoluted with the IRF.

**Syntheses.** The compounds 1,4-dibromo-2,5-bis(2-ethylhexyloxy)-3,6-bis(methylsulfinyl)benzene (**1**) and 2,10-bis(trimethyltin)-4,8,12,16-tetrakis(2-ethylhexyl)-6,14-dialkoxybenzo[1″,2″:2,3-*b*;4″,5″:2′,3′-*b*′]dithieno[2,3-*b*;2′,3′-*b*′]bis(benzo[1,2-*b*:4,5-*b*′]-dithiophene) (**7**) were synthesized according to reported procedures.[34]

*Compound* ***2a***. Compound **1** (1.00 g, 1.62 mmol) was weighed into a 100 mL round-bottom flask. 2-Trimethyltin-5-triisopropylsilylthiophene (0.652 g, 1.62 mmol) and $Pd(PPh_3)_4$ (80 mg) were added. The flask was evacuated and protected with argon, and then toluene (50 mL) was added. The reaction was carried out at 100 °C for 12 h, after which the solution was diluted with dichloromethane and passed through Celite. The solvent was removed, and the crude product was purified through chromatography on silica gel with hexanes/ethyl acetate (6/1) to give the final product **2a** (0.829 g, 65%) as a pale-yellow oil. $^1$H NMR ($CDCl_3$, 500 MHz): $\delta$ 0.67−0.98 (12H, m), 1.11−1.15 (18H, m), 1.20−2.08 (21H, m), 2.93−3.09 (6H, m), 3.45−4.30 (4H, m), 7.13−7.17 (1H, m), 7.24−7.27 (1H, m). $^{13}$C NMR: $\delta$ 10.76, 10.78, 10.94, 10.97, 11.00, 11.28, 11.32, 11.34, 11.86, 11.89, 14.14, 14.16, 12.22, 14.24, 18.67, 18.69, 18.74, 23.13, 23.14, 23.22, 23.26, 23.53, 23.55, 28.81, 28.91, 28.95, 28.98, 29.04, 29.14, 29.16, 29.82, 29.94, 29.99, 30.04, 30.12, 30.13, 38.55, 38.57, 38.61, 38.63, 38.78, 38.81, 38.97, 39.62, 39.64, 40.04, 40.07, 40.17, 79.42, 79.49, 79.70, 79.79, 80.07, 118.12, 119.81, 119.86, 130.85, 131.20, 131.22, 131.24, 131.28, 135.07, 135.53, 137.15, 137.26, 137.43, 137.50, 141.27, 141.33, 141.39, 143.76, 143.79, 153.04, 153.09, 153.14, 153.38, 153.40, 153.66, 154.10, 154.21. MALDI: calcd, 776.1; found, 776.1.

*Compound* ***2b***. By means of the same procedure as for **2a** but with **1** (0.70 g, 1.13 mmol) and 2-trimethyltin-6-triisopropylsilyl-4,8-bis(2-ethylhexyloxy)benzo[1,2-*b*:4,5-*b*′]dithiophene (0.87 g, 1.13 mmol), **2b** was obtained as a bright-yellow oil (0.38 g, 0.34 mmol, 30%). $^1$H NMR ($CDCl_3$, 500 MHz): $\delta$ 0.54−0.69 (6H, m), 0.90−1.02 (24H, m),


DOI: 10.1021/jacs.5b10175
J. Am. Chem. Soc. 2016, 138, 868−875

1.17−1.19 (18H, d, $J$ = 7.5 Hz), 1.34−2.10 (33H, m), 3.02−3.15 (6H, m), 3.64−4.34 (8H, m), 7.39−7.41 (1H, d, br), 7.64 (1H, s). $^{13}$C NMR: $\delta$ 10.96, 11.01, 11.32, 11.33, 11.41, 11.43, 11.94, 13.86, 13.93, 13.94, 14.22, 14.23, 14.25, 18.72, 18.72, 22.89, 22.97, 23.22, 23.23, 23.24, 23.25, 23.29, 23.57, 23.94, 24.01, 28.92, 28.95, 28.98, 29.14, 29.15, 29.34, 29.39, 29.40, 29.82, 29.91, 30.16, 30.53, 30.67, 30.69, 38.92, 29.99, 40.11, 40.74, 40.76, 75.98, 76.06, 79.78, 80.12, 80.49, 120.72, 123.69, 128.60, 130.00, 130.44, 130.78, 130.81, 131.89, 131.94, 133.90, 133.94, 137.72, 137.81, 141.70, 141.83, 143.83, 143.89, 143.91, 144.67, 153.24 (m), 153.48 (m). MALDI: calcd, 1136.5; found, 1137.1.

*Compound 4*. Compound **2a** (0.20 g, 0.16 mmol) was weighed into a 100 mL round-bottom flask. 2,6-Bis(trimethyltin)-4,8-bis(2-ethylhexyloxy)benzo[1,2-*b*:4,5-*b*′]dithiophene (BDT-ditin) (0.063 g, 0.081 mmol) and $Pd(PPh_3)_4$ (11 mg) were added. The flask was evacuated and protected with argon, and then toluene (8 mL) was added. The reaction was carried out at 100 °C for 12 h, after which the solution was diluted with dichloromethane and passed through Celite. The solvent was removed, and the crude product was purified through chromatography on silica gel with hexanes/ethyl acetate (6/1) to give the final product **4** (0.11 g, 0.060 mmol, 74%) as a golden-yellow oil. $^1$H NMR ($CDCl_3$, 500 MHz): $\delta$ 0.45−1.06 (50H, m), 1.11−1.15 (18H, m), 1.22−1.98 (46H, m), 2.95−3.15 (6H, m), 3.36−3.72 (4H, m), 3.96−4.30 (8H, m), 7.18−7.30 (4H, m), 7.45−7.50 (2H, m, br). $^{13}$C NMR: $\delta$ 10.57, 10.69, 10.85, 10.92, 10.97, 11.02, 11.42, 11.43, 11.85, 11.88, 11.89, 14.02, 14.07, 14.09, 14.13, 14.14, 14.22, 14.25, 18.67, 18.68, 18.69, 18.71, 22.94, 22.96, 23.06, 23.09, 23.15, 23.18, 23.20, 23.23, 23.28, 23.54, 23.90, 24.79, 28.56, 28.67, 28.77, 28.81, 28.88, 29.01, 29.05, 29.28, 29.30, 29.33, 29.76, 29.80, 29,89, 30.52, 36.74, 38.46, 38.75, 39.46, 39.94, 40.74, 40.76, 76.34, 79.44, 80.06, 80.16, 123.22, 123.72, 130.77, 130.90, 131.02, 131.29, 131.45, 131.52, 133.08, 133.22, 133.28, 137.15, 137.42, 137.64, 137.84, 138.06, 142.90, 142.94, 143.26, 143.49, 144.39, 153.88, 153.96. MALDI: calcd, 1837.0; found, 1838.0.

*Compound 6*. By means of the same procedure as for **4** but with **2b** (0.38 g, 0.34 mmol) and BDT-ditin (0.13 g, 0.17 mmol), **6** was obtained as a golden-yellow oil (0.36 g, 0.14 mmol, 85%). $^1$H NMR ($CDCl_3$, 500 MHz): $\delta$ 0.46−0.60 (12H, m), 0.62−0.80 (18H, m), 0.82−0.94 (12H, m), 0.94−0.98 (24H, m), 1.00−1.08 (24H, m), 1.18−1.19 (36H, d, $J$ = 7.5 Hz), 1.38−1.48 (40H, m), 1.58−1.64 (12H, m), 1.64−1.76 (8H, m), 1.78−1.86 (6H, m), 3.08−3.24 (12H, m), 3.58−3.74 (4H, m), 4.12−4.28 (16H, m), 7.27−7.53 (4H, m), 7.65 (2H, m). $^{13}$C NMR: $\delta$ 10.72, 10.79, 10.92, 11.04, 11.07, 11.44, 11.46, 11.50, 11.74, 11.96, 12.18, 13.83, 13.84, 14.01, 14.05, 14.09, 14.12, 14.26, 14.27, 18.74, 18.75, 22.77, 22.88, 22.91, 22.99, 23.07, 23.12, 23.14, 23.22, 23.25, 23.35, 23.95, 23.99, 24.04, 28.81, 28.87, 28.89, 28.92, 29.17, 29.36, 29.38, 29.41, 29.45, 29.72, 29.78, 29.82, 30.05, 30.06, 30.59, 30.61, 30.71, 30.74, 31.03, 31.71, 36.74, 38.79, 39.24, 39.30, 39.44, 39.88, 40.04, 40.79, 40.83, 75.96, 75.98, 76.04, 76.07, 79.77, 80.60, 123.31, 123.40, 123.92, 126.53, 128.66, 128.71, 129.81, 130.17, 130.87, 130.96, 131.35, 131.47, 131.57, 132.44, 132.67, 133.20, 133.97, 137.57, 137.78, 143.30, 143.45, 143.50, 143.52, 143.62, 144.47, 144.68, 144.71, 154.08, 154.17, 154.29. MALDI: calcd, 2559.4; found, 2560.7.

*Compound 8*. By means of the same procedure as for **4** but with **2b** (0.17 g, 0.15 mmol) and **7** (0.12 g, 0.073 mmol), **8** was obtained as a golden-yellow oil (0.17 g, 0.049 mmol, 68%). $^1$H NMR ($CDCl_3$, 500 MHz): $\delta$ 0.46−0.59 (12H, m), 0.68−0.80 (12H, m), 0.80−0.94 (12H, m), 0.94−1.18 (76H, m), 1.18−1.20 (36H, d, $J$ = 7.5 Hz), 1.48−1.58 (60H, m), 1.64−1.94 (40H, m), 2.11−2.38 (4H, m), 3.10−3.24 (12H, m), 3.60−3.78 (4H, m), 4.12−4.42 (24H, m), 7.45−7.75 (6H, m). $^{13}$C NMR: $\delta$ 10.81, 11.00, 11.02, 11.04, 11.07, 11.36, 11.42, 11.45, 11.46, 11.47, 11.49, 11.53, 11.97, 13.84, 13.86, 13.92, 14.00, 14.09, 14.23, 14.26, 14.28, 14.30, 14.35, 14.39, 18.74, 18.75, 22.77, 22.82, 22.89, 22.92, 22.94, 22.9, 23.06, 23.10, 23.25, 23.31, 23.32, 23.35, 23.93, 23.98, 24.01, 24.05, 24.08, 28.83, 28.89, 28.93, 29.40, 29.42, 29.45, 29.72, 30.03, 30.17, 30.55, 30.58, 30.61, 30.72, 30.75, 31.71, 38.84, 39.91, 39.96, 40.04, 40.10, 40.80, 40.83, 40.93, 53.53, 75.99, 76.08, 76.52, 76.61, 76.74, 77.10, 79.77, 80.60, 123.60, 123.97, 124.10, 125.47, 125.66, 126.16, 128.66, 129.83, 129.89, 130.29, 130.34, 130.70, 130.88, 130.96, 132.07, 132.22, 132.46, 132.74, 132.90, 133.23, 133.35, 133.58, 133.88, 133.96, 133.99, 137.63, 137.81, 143.32, 143.38, 143.46, 143.52, 143.60, 143.70, 144.64, 144.72, 145.49, 145.56, 154.09, 154.42, 154.48, 154.55. MALDI: calcd, 3399.5; found, 3400.5.

***FBT-11R***. Compound **4** (0.11g, 0.060 mmol) was put in a 100 mL flask, and then $P_2O_5$ (0.28 g) was added quickly. The mixture was suspended in trifluoroacetic acid (10 mL) and stirred at room temperature for 16 h. Then it was poured into 100 mL of crushed ice and stirred vigorously to afford a golden-yellow solid. The solid was filtered, dried, and dissolved in pyridine (15 mL). The resulting solution was refluxed for 12 h and then poured into 6 N HCl solution. After extraction with dichloromethane, the organic solutions were combined and dried over sodium sulfate. After that, the solvent was removed, and the residue was dissolved in THF (15 mL). To this solution was added a tetrabutylammonium fluoride solution (1 M, 1.2 mL) dropwise, and the resulting mixture was kept at room temperature for 4 h. The solvent was removed, and the product was purified by chromatography on silica gel with hexanes/dichloromethane (3/1) to afford the title compound **FBT-11R** (0.038 g, 0.027 mmol, 46%) as bright-yellowish-green gel. $^1$H NMR ($CDCl_3$, 500 MHz): $\delta$ 0.92−0.98 (18H, m), 1.08−1.14 (18H, m), 1.40−1.52 (24H, m), 1.56−1.90 (24H, m), 2.08−2.26 (6H, m), 4.31−4.34 (8H, m), 4.38−4.39 (4H, d, $J$ = 6 Hz), 7.35−7.36 (2H, d, $J$ = 5.5 Hz), 7.60−7.61 (2H, d, $J$ = 5.5 Hz). $^{13}$C NMR: $\delta$ 11.38, 11.39, 11.41, 11.44, 11.56, 19.31, 19.88, 22.81, 22.85, 23.21, 23.32, 23.38, 23.91, 27.74, 27.88, 29.40, 29.46, 29.52, 29.65, 29.82, 29.86, 29.89, 30.19, 30.31, 30.44, 30.51, 30.56, 31.74, 32.09, 32.90, 37.25, 40.95, 41.02, 71.95, 76.33, 120.05, 125.68, 126.00, 128.75, 129.00, 129.84, 130.24, 132.44, 132.53, 143.95, 144.45. Calcd MW for $C_{78}H_{106}O_6S_8$, 1394.5755. Found: MALDI-TOF MS, 1394.86; HRMS, 1394.5772.

***FBT-15R***. By means of the same procedure as for **FBT-11R** but with **6** (0.15 g, 0.060 mmol), **FBT-15R** was obtained as a bright-green gel (0.066 g, 0.031 mmol, 52%). $^1$H NMR ($CDCl_3$, 500 MHz): $\delta$ 0.84−0.92 (12H, m), 0.96−1.02 (30H, m), 1.08−1.20 (36H, m), 1.42−1.54 (40H, m), 1.62−1.94 (44H, m), 2.12−2.28 (8H, m), 4.24−4.42 (20H, m), 7.43−7.44 (2H, d, $J$ = 5 Hz), 7.54−7.55 (2H, d, $J$ = 5 Hz). $^{13}$C NMR: $\delta$ 11.39, 11.41, 11.42, 11.47, 11.53, 11.54, 14.27, 14.34, 22.81, 22.86, 23.30, 23.37, 23.93, 24.03, 29.41, 29.46, 29.50, 29.53, 29.83, 29.87, 29.90, 30.54, 30.58, 30.65, 31.75, 32.09, 40.93, 40.95, 40.98, 76.46, 77.08, 120.80, 125.92, 126.55, 129.18, 130.25, 130.32, 132.08, 132.39, 132.47, 133.03, 144.32, 144.43, 144.49, 145.18. Calcd MW for $C_{122}H_{174}O_{10}S_{10}$: 2119.0314. Found: MALDI-TOF MS, 2119.36; HRMS, 2119.0286.

***FBT-21R***. By means of the same procedure as for **FBT-11R** but with **8** (0.12 g, 0.049 mmol), **FBT-21R** was obtained as a bright-green gel (0.030 g, 0.010 mmol, 20%). $^1$H NMR ($C_2D_2Cl_4$, 500 MHz, 303K): $\delta$ 0.90 (42H, br), 1.08 (42H, br), 1.30−1.48 (60H, br), 1.57−1.82 (54H, m), 2.04−2.15 (12H, br), 4.19−4.36 (28H, m), 7.38 (2H, br), 7.46 (2H, br). $^{13}$C NMR: $\delta$ 11.40, 11.54, 14.28, 14.36, 19.88, 22.85, 23.30, 23.40, 23.86, 24.00, 26.85, 27.24, 29.40, 29.49, 29.86, 30.19, 30.31, 30.52, 32.08, 32.90, 37.25, 40.92, 76.32, 120.80, 126.10, 128.40, 130.40, 132.39, 144.38. Calcd MW for $C_{170}H_{242}O_{14}S_{14}$: 2955.4315. Found: MALDI-TOF MS, 2955.63; HRMS, 2955.4415.

## ■ ASSOCIATED CONTENT

### Supporting Information

The Supporting Information is available free of charge on the ACS Publications website at DOI: 10.1021/jacs.5b10175.

Synthesis details, characterization data, and additional information (PDF)

## ■ AUTHOR INFORMATION


### Corresponding Authors

*tgoodson@umich.edu

*lupingyu@uchicago.edu


### Notes

The authors declare no competing financial interest.



DOI: 10.1021/jacs.5b10175
J. Am. Chem. Soc. 2016, 138, 868−875

## ■ ACKNOWLEDGMENTS

This work was mainly supported by the NSF (CHE-1503852) and also benefited from the NSF MRSEC at the University of Chicago.

## ■ REFERENCES

(1) Payne, M. M.; Parkin, S. R.; Anthony, J. E.; Kuo, C. C.; Jackson, T. N. *J. Am. Chem. Soc.* **2005**, *127*, 4986.
(2) Jones, B. A.; Facchetti, A.; Wasielewski, M. R.; Marks, T. J. *J. Am. Chem. Soc.* **2007**, *129*, 15259.
(3) Grimsdale, A. C.; Müllen, K. *Macromol. Rapid Commun.* **2007**, *28*, 1676.
(4) Huang, H. H.; Prabhakar, C.; Tang, K. C.; Chou, P. T.; Huang, G. J.; Yang, J. S. *J. Am. Chem. Soc.* **2011**, *133*, 8028.
(5) Yuan, S. W.; Kirklin, S.; Dorney, B.; Liu, D. J.; Yu, L. P. *Macromolecules* **2009**, *42*, 1554.
(6) Durban, M. M.; Kazarinoff, P. D.; Segawa, Y.; Luscombe, C. K. *Macromolecules* **2011**, *44*, 4721.
(7) Grimsdale, A. C.; Müllen, K. In *Design and Synthesis of Conjugated Polymers*; Leclerc, M., Morin, J.-F., Eds.; Wiley-VCH: Weinheim, Germany, 2010; Chapter 7.
(8) Zheng, Q.; Jung, B. J.; Sun, J.; Katz, H. E. *J. Am. Chem. Soc.* **2010**, *132*, 5394.
(9) Wang, B.; Forster, M.; Preis, E.; Wang, H.; Ma, Y.; Scherf, U. *J. Polym. Sci., Part A: Polym. Chem.* **2009**, *47*, 5137.
(10) Yu, L.; Chen, M.; Dalton, L. R. *Chem. Mater.* **1990**, *2*, 649.
(11) Simpson, C. D.; Brand, J. D.; Berresheim, A. J.; Przybilla, L.; Rader, H. J.; Müllen, K. *Chem. - Eur. J.* **2002**, *8*, 1424.
(12) Wu, J.; Tomović, Ž.; Enkelmann, V.; Müllen, K. *J. Org. Chem.* **2004**, *69*, 5179.
(13) Takeya, J.; Goldmann, C.; Haas, S.; Pernstich, K. P.; Ketterer, B.; Batlogg, B. *J. Appl. Phys.* **2003**, *94*, 5800.
(14) Tour, J. M.; Lamba, J. J. S. *J. Am. Chem. Soc.* **1993**, *115*, 4935.
(15) Goldfinger, M. B.; Swager, T. M. *J. Am. Chem. Soc.* **1994**, *116*, 7895.
(16) Lamba, J. J. S.; Tour, J. M. *J. Am. Chem. Soc.* **1994**, *116*, 11723.
(17) Hasegawa, T.; Takeya, J. *Sci. Technol. Adv. Mater.* **2009**, *10*, 024314.
(18) Jurchescu, O. D.; Popinciuc, M.; van Wees, B. J.; Palstra, T. T. M. *Adv. Mater.* **2007**, *19*, 688.
(19) Takimiya, K.; Osaka, I.; Mori, T.; Nakano, M. *Acc. Chem. Res.* **2014**, *47*, 1493.
(20) Minemawari, H.; Yamada, T.; Matsui, H.; Tsutsumi, J.; Haas, S.; Chiba, R.; Kumai, R.; Hasegawa, T. *Nature* **2011**, *475*, 364.
(21) Haas, S.; Takahashi, Y.; Takimiya, K.; Hasegawa, T. *Appl. Phys. Lett.* **2009**, *95*, 022111.
(22) Li, J.; Zhang, Q. *ACS Appl. Mater. Interfaces* **2015**, *7*, 28049.
(23) Wang, C.; Zhang, J.; Long, G.; Aratani, N.; Yamada, H.; Zhao, Y.; Zhang, Q. *Angew. Chem., Int. Ed.* **2015**, *54*, 6292.
(24) Anthony, J. E. *Chem. Rev.* **2006**, *106*, 5028.
(25) Anthony, J. E. *Angew. Chem., Int. Ed.* **2008**, *47*, 452.
(26) Bendikov, M.; Wudl, F.; Perepichka, D. F. *Chem. Rev.* **2004**, *104*, 4891.
(27) Qiu, S.; Lu, P.; Liu, X.; Shen, F.; Liu, L.; Ma, Y.; Shen, J. *Macromolecules* **2003**, *36*, 9823.
(28) Mancuso, A. J.; Swern, D. *Synthesis* **1981**, *1981*, 165.
(29) Sirringhaus, H.; Friend, R. H.; Wang, C.; Leuninger, J.; Müllen, K. *J. Mater. Chem.* **1999**, *9*, 2095.
(30) Gao, P.; Feng, X.; Yang, X.; Enkelmann, V.; Baumgarten, M.; Müllen, K. *J. Org. Chem.* **2008**, *73*, 9207.
(31) Gao, P.; Beckmann, D.; Tsao, H. N.; Feng, X.; Enkelmann, V.; Baumgarten, M.; Pisula, W.; Müllen, K. *Adv. Mater.* **2009**, *21*, 213.
(32) Gao, P.; Cho, D.; Yang, X.; Enkelmann, V.; Baumgarten, M.; Müllen, K. *Chem. - Eur. J.* **2010**, *16*, 5119.
(33) Oyaizu, K.; Iwasaki, T.; Tsukahara, Y.; Tsuchida, E. *Macromolecules* **2004**, *37*, 1257.
(34) Zheng, T.; Lu, L.; Jackson, N. E.; Lou, S. J.; Chen, L. X.; Yu, L. *Macromolecules* **2014**, *47*, 6252.
(35) Xiao, K.; Liu, Y.; Qi, T.; Zhang, W.; Wang, F.; Gao, J.; Qiu, W.; Ma, Y.; Cui, G.; Chen, S.; Zhan, X.; Yu, G.; Qin, J.; Hu, W.; Zhu, D. *J. Am. Chem. Soc.* **2005**, *127*, 13281.
(36) Payne, M. M.; Parkin, S. R.; Anthony, J. E. *J. Am. Chem. Soc.* **2005**, *127*, 8028.
(37) Mondal, R.; Tönshoff, C.; Khon, D.; Neckers, D. C.; Bettinger, H. F. *J. Am. Chem. Soc.* **2009**, *131*, 14281.
(38) Anand, S.; Varnavski, O.; Marsden, J. A.; Haley, M. M.; Schlegel, H. B.; Goodson, T., 3rd *J. Phys. Chem. A* **2006**, *110*, 1305.
(39) Norris, B. N.; Zhang, S.; Campbell, C. M.; Auletta, J. T.; Calvo-Marzal, P.; Hutchison, G. R.; Meyer, T. Y. *Macromolecules* **2013**, *46*, 1384.
(40) Park, Y. I.; Kuo, C. Y.; Martinez, J. S.; Park, Y. S.; Postupna, O.; Zhugayevych, A.; Kim, S.; Park, J.; Tretiak, S.; Wang, H. L. *ACS Appl. Mater. Interfaces* **2013**, *5*, 4685.
(41) Peeters, E.; van Hal, P. A.; Knol, J.; Brabec, C. J.; Sariciftci, N. S.; Hummelen, J. C.; Janssen, R. A. J. *J. Phys. Chem. B* **2000**, *104*, 10174.
(42) Ritzert, N. L.; Truong, T.-T.; Coates, G. W.; Abruña, H. D. *J. Phys. Chem. C* **2014**, *118*, 924.
(43) Facchetti, A.; Yoon, M.-H.; Stern, C. L.; Hutchison, G. R.; Ratner, M. A.; Marks, T. J. *J. Am. Chem. Soc.* **2004**, *126*, 13480.
(44) Martin, R. E.; Diederich, F. *Angew. Chem., Int. Ed.* **1999**, *38*, 1350.
(45) Mori, T.; Nishimura, T.; Yamamoto, T.; Doi, I.; Miyazaki, E.; Osaka, I.; Takimiya, K. *J. Am. Chem. Soc.* **2013**, *135*, 13900.
(46) Niimi, K.; Shinamura, S.; Osaka, I.; Miyazaki, E.; Takimiya, K. *J. Am. Chem. Soc.* **2011**, *133*, 8732.
(47) Okamoto, T.; Kudoh, K.; Wakamiya, A.; Yamaguchi, S. *Chem. - Eur. J.* **2007**, *13*, 548.
(48) Wex, B.; Kaafarani, B. R.; Danilov, E. O.; Neckers, D. C. *J. Phys. Chem. A* **2006**, *110*, 13754.
(49) Reynolds, G. A.; Drexhage, K. H. *Opt. Commun.* **1975**, *13*, 222.
(50) Wex, B.; Jradi, F. M.; Patra, D.; Kaafarani, B. R. *Tetrahedron* **2010**, *66*, 8778.
(51) Bhaskar, A.; Ramakrishna, G.; Lu, Z.; Twieg, R.; Hales, J. M.; Hagan, D. J.; Van Stryland, E.; Goodson, T., 3rd *J. Am. Chem. Soc.* **2006**, *128*, 11840.
(52) Ramakrishna, G.; Bhaskar, A.; Goodson, T., 3rd *J. Phys. Chem. B* **2006**, *110*, 20872.
(53) Lee, D. I.; Goodson, T., 3rd *J. Phys. Chem. B* **2006**, *110*, 25582.
(54) Xu, C.; Webb, W. W. *J. Opt. Soc. Am. B* **1996**, *13*, 481.
(55) Liu, Z. Q.; Fang, Q.; Wang, D.; Cao, D. X.; Xue, G.; Yu, W. T.; Lei, H. *Chem. - Eur. J.* **2003**, *9*, 5074.
(56) Bhaskar, A.; Guda, R.; Haley, M. M.; Goodson, T., 3rd *J. Am. Chem. Soc.* **2006**, *128*, 13972.
(57) Hohenau, A.; Cagran, C.; Kranzelbinder, G.; Scherf, U.; Leising, G. *Adv. Mater.* **2001**, *13*, 1303.
(58) *Photoresponsive Polymers II*; Marder, S. R., Lee, K.-S., Eds.; Springer: Berlin, 2008.
(59) Ogawa, K. *Appl. Sci.* **2014**, *4*, 1.
(60) Tang, C.; Zheng, Q.; Zhu, H.; Wang, L.; Chen, S.-C.; Ma, E.; Chen, X. *J. Mater. Chem. C* **2013**, *1*, 1771.
(61) Pommerehne, J.; Vestweber, H.; Guss, W.; Mahrt, R. F.; Bassler, H.; Porsch, M.; Daub, J. *Adv. Mater.* **1995**, *7*, 551.
(62) Frisch, M. J.; Trucks, G. W.; Schlegel, H. B.; Scuseria, G. E.; Robb, M. A.; Cheeseman, J. R.; Scalmani, G.; Barone, V.; Mennucci, B.; Petersson, G. A.; Nakatsuji, H.; Caricato, M.; Li, X.; Hratchian, H. P.; Izmaylov, A. F.; Bloino, J.; Zheng, G.; Sonnenberg, J. L.; Hada, M.; Ehara, M.; Toyota, K.; Fukuda, R.; Hasegawa, J.; Ishida, M.; Nakajima, T.; Honda, Y.; Kitao, O.; Nakai, H.; Vreven, T.; Montgomery, J. A., Jr.; Peralta, J. E.; Ogliaro, F.; Bearpark, M.; Heyd, J. J.; Brothers, E.; Kudin, K. N.; Staroverov, V. N.; Kobayashi, R.; Normand, J.; Raghavachari, K.; Rendell, A.; Burant, J. C.; Iyengar, S. S.; Tomasi, J.; Cossi, M.; Rega, N.; Millam, J. M.; Klene, M.; Knox, J. E.; Cross, J. B.; Bakken, V.; Adamo, C.; Jaramillo, J.; Gomperts, R.; Stratmann, R. E.; Yazyev, O.; Austin, A. J.; Cammi, R.; Pomelli, C.; Ochterski, J. W.; Martin, R. L.; Morokuma, K.; Zakrzewski, V. G.; Voth, G. A.; Salvador, P.; Dannenberg, J. J.; Dapprich, S.; Daniels, A. D.; Farkas, Ö.;



DOI: 10.1021/jacs.5b10175
*J. Am. Chem. Soc.* 2016, 138, 868−875

Foresman, J. B.; Ortiz, J. V.; Cioslowski, J.; Fox, D. J. *Gaussian 09*, revision A.02; Gaussian, Inc.: Wallingford, CT, 2009.
(63) Adegoke, O. O.; Jung, I. H.; Orr, M.; Yu, L.; Goodson, T., 3rd *J. Am. Chem. Soc.* **2015**, *137*, 5759.
(64) Varnavski, O.; Abeyasinghe, N.; Arago, J.; Serrano-Perez, J. J.; Orti, E.; Lopez Navarrete, J. T.; Takimiya, K.; Casanova, D.; Casado, J.; Goodson, T., 3rd *J. Phys. Chem. Lett.* **2015**, *6*, 1375.
(65) Yau, S. H.; Varnavski, O.; Gilbertson, J. D.; Chandler, B.; Ramakrishna, G.; Goodson, T. *J. Phys. Chem. C* **2010**, *114*, 15979.



DOI: 10.1021/jacs.5b10175
*J. Am. Chem. Soc.* 2016, 138, 868−875